

Article

Development of an Active Equalizer for Lithium-Ion Batteries

Zong-Zhen Yang

Department of Electrical Engineering, Ming Chi University of Technology, No. 84, Gungjuan Road, Taishan District, New Taipei City 24301, Taiwan; y913023@gmail.com; Tel.: +886-2-2908-9899

Abstract: In this paper, a bi-directional-buck-boost-converter-based active equalizer is developed. The energy between adjacent cells can be transferred bi-directionally by manipulating the balancing current to solve the unbalanced problem in a battery module. It is noted that the conduction time of the main switch in the conventional buck-boost equalizer is fixed. Thus, the balancing current will diminish as the voltage difference of the adjacent cells decreases, which results in a prolonged equilibrium period. This paper has proposed two methods, namely, the varied-on-time (VOT) method and the voltage ratio modulation (VRM) method, to shorten the equilibrium period. In the VOT method, the conduction time of the main switch is determined according to high state-of-charge (SOC) cell voltage. In this way, the balancing current is able to be kept at the desired level rather than reduced during the balancing process. On the other hand, the VRM method computes the proportion of the conduction time and the cut-off time in a switching cycle based on the voltages of adjacent cells. Hence, the equalizer can deliver the maximum energy in a switching period and shorten the equilibrium period. The simulation platform and experiments with four batteries connected in serial are carried out to verify the proposed control methods. According to the experimental results, the VOT method saves 10.3%, 11.7%, and 16% of the equilibrium time compared with the fixed duty cycle (FDC) method. The VRM method can shorten 35.9%, 36.6%, and 37.3% of the equilibrium time compared with the FDC method.

Keywords: active equalizer; bi-directional buck-boost converter; varied-on-time method; voltage ratio modulation method



Citation: Yang, Z.-Z. Development of an Active Equalizer for Lithium-Ion Batteries. *Electronics* **2022**, *11*, 2219. <https://doi.org/10.3390/electronics11142219>

Academic Editor: M. Tariq Iqbal

Received: 17 June 2022

Accepted: 13 July 2022

Published: 15 July 2022

Publisher's Note: MDPI stays neutral with regard to jurisdictional claims in published maps and institutional affiliations.



Copyright: © 2022 by the author. Licensee MDPI, Basel, Switzerland. This article is an open access article distributed under the terms and conditions of the Creative Commons Attribution (CC BY) license (<https://creativecommons.org/licenses/by/4.0/>).

1. Introduction

With rapid economic development, population growth, and the emissions from internal combustion engine vehicles, the issues of energy shortage and global warming have emerged gradually. Therefore, energy-saving and eco-friendly measures have become highly valued. In recent years, the governments of many countries have developed incentives for electric vehicles and implemented energy subsidy reforms. In this background, the application of secondary batteries is rising as the global trend. Secondary batteries can be categorized by their chemical characteristics into lead-acid batteries, NI-MH batteries (nickel-metal hydride batteries), NiCd batteries (nickel-cadmium batteries), and Li-ion batteries (lithium-ion batteries). In the application of electric vehicles and smart grids, a high power/high voltage is required for long-term operation. Therefore, lithium-ion batteries, featuring high energy density, no memory effect, and low self-discharge rate, have been widely utilized in electric vehicles and household storage systems [1–4]. Due to the low voltage and insufficient capacity of a single cell, lithium-ion batteries are usually connected in series and in parallel as a battery pack or battery module to meet the demands of high power and large capacity for energy storage systems or electric vehicles [5–9]. However, there are some deviations in the batteries during the manufacturing process, leading to a slight difference in chemical characteristics and electrical properties among cells. In addition, distinct operating temperature, self-discharging rate, and aging degradation will cause unbalance in a battery module when repeatedly charging and discharging. It may result in problems in reliability and safety and may lower the energy utilization of the

battery pack. In addition, the unbalance of the battery module may increase replacement and maintenance cost, etc. [10–12]. To solve the above issues, the usage of an equalizer could keep the battery module balance, improve energy utilization, and further prolong the life span of the battery module [13–15].

Conventionally, in order to reduce imbalance among batteries, the characteristics of individual cells are measured in advance. Then, cells with similar properties are selected and constructed as a module [16]. Nowadays, various balancing structures and corresponding control techniques have been developed to achieve balance among cells effectively. According to the energy balancing mechanism, these techniques can be divided into passive balancing and active balancing [17–21]. In passive balancing, the resistance and switch are connected with each battery cell in parallel. The surplus energy of a high-SOC cell dissipates via resistance until it is equal to that of a low-SOC cell. This method has the advantages of low cost, simple structure, and being easy to control, but its balancing process takes a longer time and causes energy consumption and heating [17,18].

The active balancing transfers energy from a high-SOC battery to a low-SOC battery to achieve balance. Thus, compared with passive balancing, it achieves better energy utilization efficiency and shortens equilibrium time. As a result, active balancing is extensively investigated nowadays [19–23]. However, due to its hardware cost, control complexity, and reliability, it is still challenging for active balancing to become a commercial product. According to the ways active equalizers perform the transfer of energy, active balancing can be classified into the forms of capacitor, inductor, transformer, and converter [19–32]. In a capacitor-based equalizer, capacitors and switches are utilized to make energy flow among the cells to achieve an active balancing. The control and structure are simple and easy to implement, but the balancing current will decrease as the voltages among cells become closer, resulting in a prolonged equilibrium time [23–25]. A converter-based equalizer can be divided into isolated converters [26,27] and non-isolated converters [28–32]. Since a converter-based equalizer uses magnetic components such as transformers or inductances as energy storage components to transfer energy, it can be designed to transfer energy from a cell to a module or from a module to a cell. As a power converter is used as a medium for energy transfer, better conversion efficiency could be achieved, but the structure and control are more complicated and the cost is also higher. As for a converter-based equalizer with an isolated transformer, it can be divided into multiple sets of a transformer and a transformer with multiple secondary windings. The design is more flexible but complex, and the total volume is relatively bulky. On the other hand, the non-isolated inductive balancing structure can be realized by a bi-directional buck-boost converter. Unlike an equalizer with a transformer, it can save space and cost. In the meantime, it improves the small balancing current in the later stage of the balancing process by the control method [28–30]. The inductor-based equalizer enables zero-voltage and zero-current switching through LC resonance; thus, higher conversion efficiency can be obtained [31,32]. The active balancing structure is widely applied in multiple batteries in series or energy storage modules due to its better design flexibility, energy utilization, and shorter balancing time than passive balancing. Therefore, this paper focuses on active balancing and adopts a bi-directional buck-boost converter as the hardware circuit of the equalizer.

This paper discusses the problem of prolonged equilibrium time caused by a decreased balancing current due to the minor difference of voltage in adjacent cells during the balancing process. The conventional control techniques cannot maintain the balancing current throughout the whole balancing process; therefore, it takes a longer time for equilibrium. In order to solve this problem, Ref. [33] proposed the adaptive varied duty cycle (AVDC) technique, which calculates the duty cycle with the terminal voltage of adjacent batteries to achieve the purpose of adjusting the balancing current. However, due to the nonlinear factors in the circuit, such as wire resistance and the on-resistance of the power switch, it may not keep the balancing current completely identical. Ref. [34] proposed the curve-fitting modulation (CFM) method to fix the balancing current. The low-SOC voltage and the voltage difference between adjacent cells are measured, and the

optimal duty cycles with twelve voltage stages are given. Then, an equation of the curve can be obtained by approaching the CFM method. Although this method can maintain the balancing current during the process, it needs practical tests and records the values of the optimal duty cycle in each battery voltage scenario in advance. If the number of test stages is larger, it will take more time conducting experiments to obtain the best curve-fitting approximation equation. Ref. [35] proposed adaptive fuzzy-logic-based balancing current control, which uses a fuzzy logic controller to adjust the duty cycle. The input parameters of the controller are the voltages of a single cell and battery stacks. The adaptive duty cycle can be acquired through fuzzification, a rule table, and a defuzzification process. This method can solve the nonlinear consideration of the system and get an accurate duty cycle. However, the membership functions and the rule table need to be designed to comply with the system specifications, and the calculation of the function is more complex so it is difficult to implement by a low-cost MCU with a simple calculation.

This paper proposes a fast active equalizer based on a bi-directional buck-boost converter and implements two adaptive balancing current control techniques. The VOT method calculates the conduction time every switching cycle by simply detecting the voltage of a high-SOC cell to maintain the balancing current in the whole balancing process. Since both the conduction time and the cut-off time in a switching period are controllable, the VRM method is presented. It uses the terminal voltage of the high SOC and the low SOC of adjacent batteries to obtain the optimal proportion of the conduction time and the cut-off time in a switching period, which is used to maximize the balancing current to shorten the equilibrium time and improve overall performance. The main contributions of this paper are as follows: The active equalizer has a simple circuit structure with a small inductance value since the converter is designed to operate in discontinuous conduction mode, which can further reduce the volume of the equalizer. The proposed control method does not require a battery-equivalent circuit model or complicated calculations. It only needs to detect the terminal voltages of the adjacent batteries to attain the proportion of the conduction time and cut-off time in a switching cycle and then maximize the balancing current during the whole balancing process. With a simple equation, a low-cost microcontroller can be utilized to implement the presented method in multi-string battery modules. Moreover, the proposed equalizer could be modularized conveniently and employed with more cells connected in series. The organization of this paper is as follows. Section 2 introduces the circuit structure and the analysis of operation principle of the equalizer. Section 3 explains the balancing control technique, deriving the equations of the balancing current, the conduction time, and the cut-off time according to the adjacent cell voltages. The simulation platform is explained and the proposed control method is verified in Section 4. Section 5 shows the experimental test platform and measurement results to demonstrate the feasibility and performance of the presented method. In the end, the conclusion of this paper is described in Section 6.

2. Hardware Structure of Equalizer and Operation Principle

The active equalizer requires not only bi-directional energy transfer but a rapid equalization process. To save equilibrium time, the current-based inductive topology is prioritized in this application [27–29]. Hence, a buck-boost converter is utilized in this paper since its structure is simple and the energy storage element is an inductor by which the balancing current can be controlled by modulating the conduction time. The circuit diagram is illustrated in Figure 1.

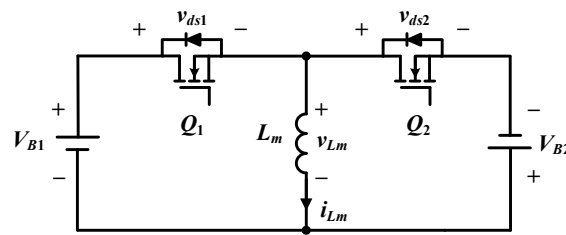


Figure 1. Bi-directional buck-boost circuit diagram.

where L_m is the energy storage inductor, Q_1 is the main switch, and the conventional diode is replaced with the switch Q_2 as a synchronized switch. The input voltage and output voltage are substituted with batteries V_{B1} and V_{B2} , respectively. This structure can be extended according to the number of batteries. By taking the number of batteries N , $(N - 1)$ sets of bi-directional buck-boost circuits should be organized to perform the equalization process. The complete circuit diagram of four series batteries is shown in Figure 2. In this structure, the balancing current that is the average input current and average output current of the batteries could be regarded as the average current of the inductor conducted in the rising time and falling time intervals, respectively. In order to improve the balance efficiency, adjusting the conduction time of the main switch can effectively regulate the balancing current at the desired value to speed up the balancing process. In addition, the circuit operated in discontinuous conduction mode (DCM) enables the controller to calculate an accurate average current by integrating the area of the inductor current waveform over one switching cycle.

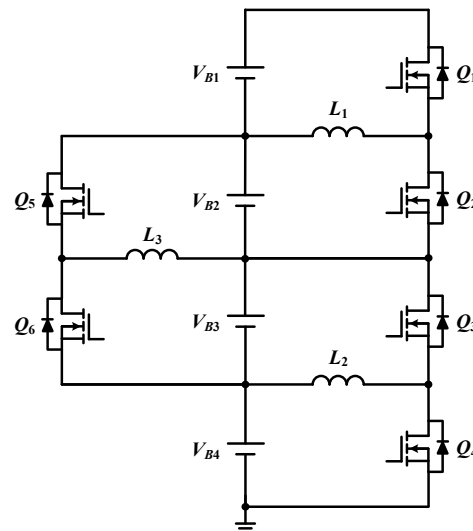


Figure 2. Equalizer circuit with four batteries.

Figure 3 shows the diagram of the energy transfer path from battery V_{B1} to battery V_{B2} (assuming the SOC of V_{B1} is higher than V_{B2}). V_{B1} stores energy in the inductor by controlling the main switch Q_1 turn-on, while the inductor current increases with slope V_{B1}/L_m , as shown in Figure 3a. The switch Q_2 is driven with the complementary signal to Q_1 . When Q_1 is turned off, Q_2 is in the conduction state. Moreover, the inductor current decreases with slope V_{B2}/L_m and releases energy to V_{B2} until the inductor current is zero. The diagram of the inductor releasing energy to V_{B2} is illustrated in Figure 3b. Vice versa, if the voltage of V_{B2} is higher than that of V_{B1} , Q_2 becomes the main switch and transfers the energy from V_{B2} to V_{B1} .

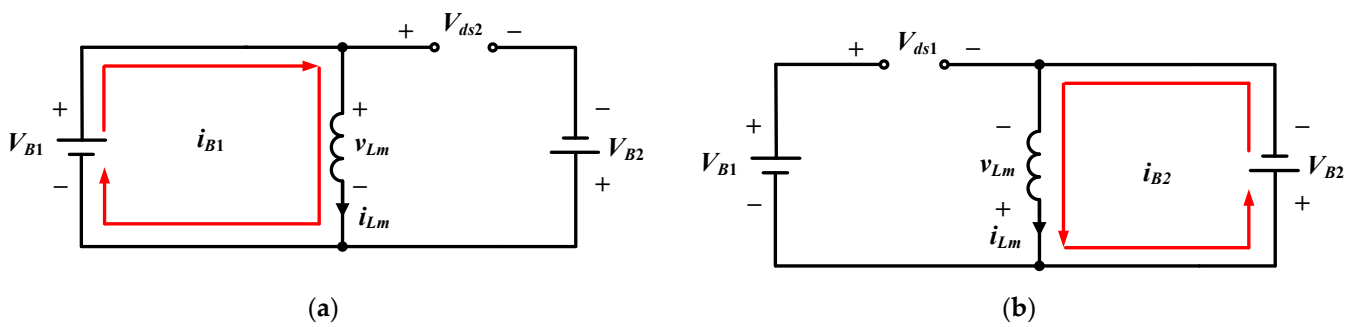


Figure 3. The energy transfer path from V_{B1} to battery V_{B2} : (a) battery V_{B1} stores energy to the inductor and (b) the inductor releases energy to battery V_{B2} .

In this study, the equalizer is designed and operated in discontinuous conduction mode (VOT method) and in critical conduction mode (VRM method). According to the concept of volt-second balance and the average voltage on the inductor over a switching cycle being zero, the equation of the designed inductor value in critical conduction mode is shown:

$$L_{mb} = \frac{V_{B2} T_S}{2I_{B2}} (1 - D)^2 \quad (1)$$

where D and T_S are the duty cycle and switching period and I_{B2} is the average current of battery V_{B2} . The inductor value should be designed with the lowest level of the battery to ensure that the equalizer operates in critical conduction mode or discontinuous conduction mode under any conditions.

3. Control Strategy of Equalizer

The main goals of the battery equalizer include high energy transfer efficiency, fast balancing speed, and safety in use. Moreover, the primary requirement is to achieve equilibrium rapidly. The key to the balancing speed is directly related to the balancing current. In the conventional control method, the duty cycle which means the conduction time of the main switch is constant as the buck-boost converter is used as an equalizer structure. Since the voltage of the high-SOC battery during the equalization process gradually decreases, the voltage difference between adjacent batteries becomes smaller so that the balancing current will drop if the conduction time does not change adaptively, resulting in a significant time cost in the equilibrium. Therefore, if the magnitude of the balancing current can be regulated according to the voltage of the battery, it could speed up the balance. In this circuit, the inductor current integrated over one switching period can be regarded as the average current from the battery while the main switch is turned on, so the balancing current can be controlled by changing the time interval of the conduction state. A concept diagram of the three strategies with balancing current control is shown in Figure 4, where i_{Lm} is the inductor current and I_{B1} is the average current of battery V_{B1} .

In Figure 4, the conventional fixed duty cycle (FDC) method does not adjust the duty cycle followed by the reduced battery voltage, so balancing current will decrease during the equilibrium process, resulting in a longer time to reach balance. The VOT method modulates the duty cycle of the main switch based on the battery voltage to maintain the magnitude of the balancing current. However, the conduction time cannot be optimized since only the voltage of the high-SOC battery is considered. To improve the balancing speed, the VRM method is proposed, which detects both the voltages of the adjacent batteries to calculate the distribution ratio of the conduction time and cut-off time of the main switch in a switching period for optimizing the energy that is stored and released by the inductor. Then, the average current can be maximized to effectively shorten the equilibrium process. The principle of control strategies is explained next.

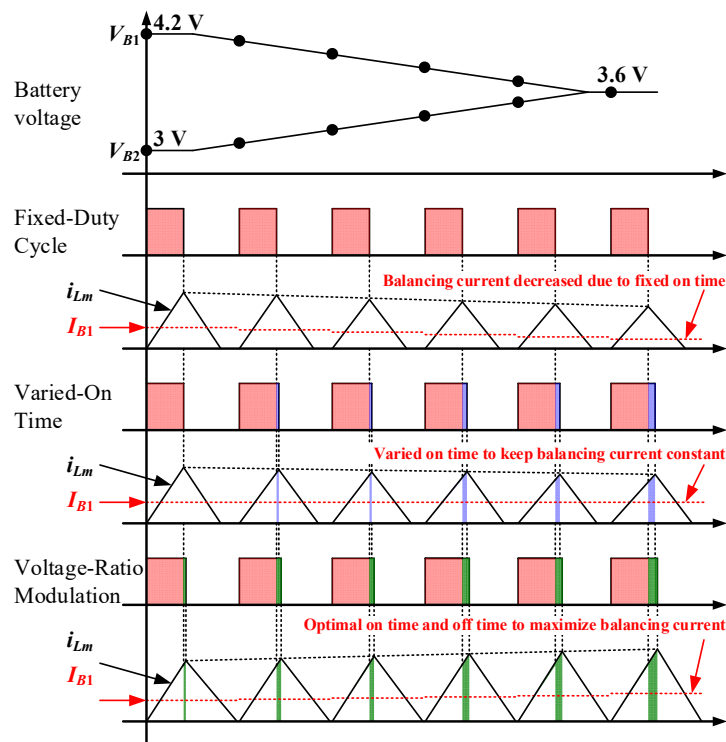


Figure 4. Comparison diagram of balancing current control strategies.

3.1. Varied-on-Time Method

The adjacent cells can transfer energy between cells by manipulating the sequence of the switching operations of the buck-boost converter. Figure 5 shows the diagram of the circuit structure and the waveform of the inductor current when the switches Q_1 and Q_2 are in conduction states sequentially. The energy of the inductor is charged when switch Q_1 is turn on as arrow in red color in Figure 5. While switch Q_2 is turn on as arrow in blue color, the energy of the inductor is released. V_{B1} and V_{B2} are the adjacent voltages of the high-SOC battery and the low-SOC battery, respectively, I_{pk} is the peak value of the inductor current, $I_{Q1,avg}$ is the average current of main switch Q_1 as well as balancing current I_{B1} of battery V_{B1} , T_{on} is the conduction time of the main switch Q_1 , and T_s is the switching period. The converter is operated in discontinuous conduction mode; hence, the inductor current will reduce to zero before the next switching cycle begins.

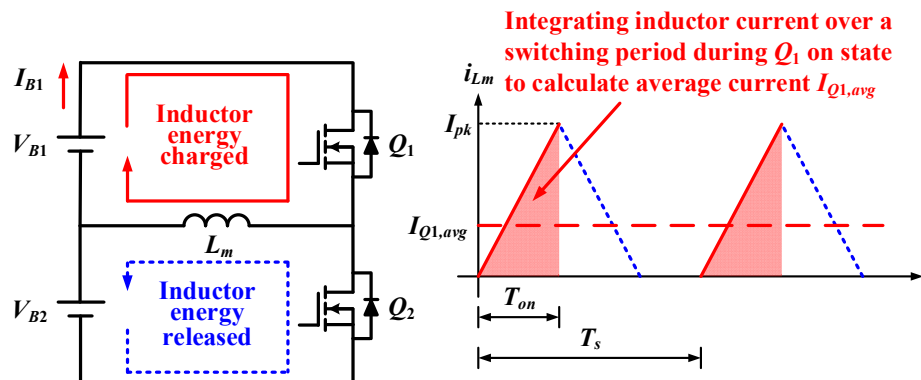


Figure 5. Circuit diagram and waveform of inductor currents.

The relation between the inductor current and the battery voltage is shown:

$$V_{B1} = \frac{L_m I_{pk}}{T_{on}} \tag{2}$$

Since the inductance is constant, it can be observed that the peak value I_{pk} of the inductor current is proportional to the battery voltage V_{B1} . The integration of the inductor current over the switching period is the output charge of battery. When entering the balancing process, the voltage V_{B1} of the high-SOC battery will become lower. If the conduction time T_{on} of the switch Q_1 is fixed, it can be seen from Equation (2) that the peak current I_{pk} will drop, which results in a prolonged equilibrium time. Hence, the VOT method is proposed to deal with this problem.

As discussed in Figure 5, the balancing current of the battery V_{B1} is the average current of the main switch Q_1 , and it is related to the peak current of the inductor, as shown below:

$$I_{Q1,avg} = I_{B1} = \frac{I_{pk}T_{on}}{2T_S} \quad (3)$$

$$T_{on} = \sqrt{\frac{2I_{B1}L_m}{V_{B1}f_S}} \quad (4)$$

Equation (4) can be derived from Equations (2) and (3). It can be seen from Equation (4) that the conduction time of the main switch Q_1 can be controlled simply by detecting the terminal voltage of the high-SOC battery. Thus, in order to maintain the balancing current I_{B1} , the conduction time T_{on} should be increased when the voltage of the high-SOC battery drops.

However, Equation (4) only detects the voltage of the high-SOC battery to calculate the conduction time of main switch Q_1 . Although it could prevent the prolonged balancing time from the balancing current decreasing due to the voltage drop, it cannot take the low-SOC battery into account to dispatch the optimal proportion of the conduction time and the cut-off time in a switching period. Therefore, this paper proposes a VRM method to optimize the conduction time and cut-off time, allowing the balancing current to be maximized based on the current battery voltage in a switching period and transferring energy from the high-SOC battery to the low-SOC battery more effectively to reduce the equilibrium time.

3.2. Voltage Ratio Modulation Method

To further increase the balancing current and achieve cell potential balance rapidly, a control strategy is proposed to effectively allocate the conduction time and cut-off time required in a complete switching period by detecting the voltages of two adjacent cells. Then, the converter is operated in critical conduction mode. With Equation (4), the relation between the conduction time and cut-off time can be written:

$$\frac{T_{on}}{T_{off}} = \sqrt{\frac{2I_{B1}L_m}{V_{B1}f_S}} / \sqrt{\frac{2I_{B2}L_m}{V_{B2}f_S}} = \sqrt{\frac{I_{B1}V_{B2}}{I_{B2}V_{B1}}} \quad (5)$$

in which T_{off} is the cut-off time of the main switch as well as the conduction time of Q_2 and I_{B2} is the balancing current of battery V_{B2} . If the components in the circuit are all ideal and there is no loss in the circuit, the input power is equal to the output power as in Equation (6). The distribution ratio of conduction time and cut-off time can be arranged by Equation (7), which is directly related to the voltages of adjacent batteries.

$$P_1 = P_2 \rightarrow V_{B1}I_{B1} = V_{B2}I_{B2} \rightarrow \frac{V_{B1}}{V_{B2}} = \frac{I_{B2}}{I_{B1}} \quad (6)$$

$$\frac{T_{on}}{T_{off}} = \frac{V_{B2}}{V_{B1}} \quad (7)$$

From Equation (7), if the voltage of battery V_{B1} is higher than that of battery V_{B2} , the conduction time of the main switch will be less than the cut-off time in a switching

period. Furthermore, the sum of the conduction time and the cut-off time is the time of the switching period, then Equations (8) and (9) can be derived, respectively.

$$T_{on} = \frac{V_{B2}}{V_{B1} + V_{B2}}(1 - \alpha)T_s \tag{8}$$

$$T_{off} = \frac{V_{B1}}{V_{B1} + V_{B2}}(1 - \alpha)T_s \tag{9}$$

since the circuit operation should consider the dead time and time delay of the main switch and synchronized switch, the conduction time and cut-off time in the switching period are both concerned with an effective factor α , selected as 0.01 in this study. By Equations (8) and (9), it can be seen that the proportion of the conduction time of Q_1 is related to the low-SOC voltage of battery V_{B2} , and the cut-off time of Q_1 is associated with the low-SOC voltage of battery V_{B1} .

Figure 6a is the flow chart of the main control software program of the equalizer. TMS320F280049 produced by TI company is selected as a digital signal processor (DSP), and its maximum clock speed is 100 MHz. In the beginning, each required module is initialized and enabled. After entering the infinite loop, it continuously communicates with the ADAM-4117 voltage-sense module to obtain the terminal voltage information of each battery and is used in the balancing program. Figure 6b shows the flow chart of the balancing process of the VOT method. Initially, it reads the information of the battery voltage and then calculates the voltage difference ΔV_{diff} between the maximum battery voltage V_{max} and the minimum voltage V_{min} . Then, the voltage difference is used to determine whether the battery balance state is reached by comparing with the critical value V_{limit} . Next, according to the aforementioned Equation (4), the conduction time is calculated in real time with the high-SOC voltage of battery condition. Furthermore, the energy flow of the converter can be controlled by the relation of the battery voltage of adjacent batteries. Figure 6c depicts the flow chart of the balancing process of the VRM method. The different portion is that when the equalizer is in the balancing process, the proportion of the conduction time and cut-off time in a switching cycle will be calculated based on Equations (8) and (9). As a result, the balancing current can be further maximized to achieve balance rapidly.

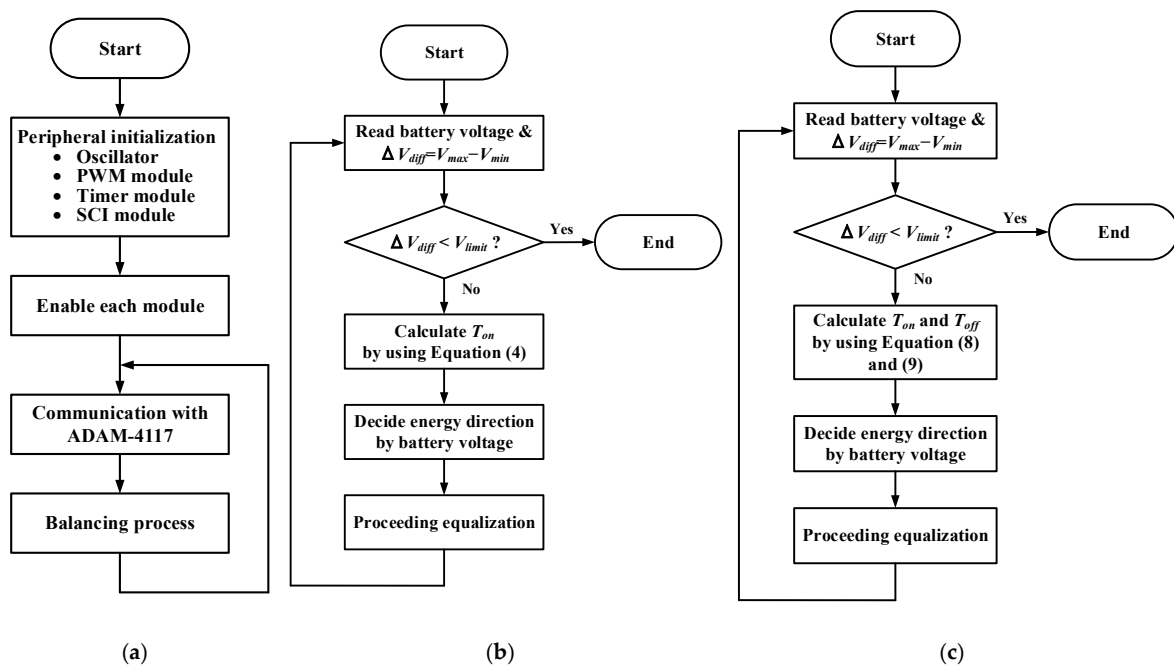


Figure 6. Software flowchart of the proposed balancing strategy: (a) main program; (b) balancing program of the VOT method; and (c) balancing program of the VRM method.

4. Simulation Results

In this section, the simulation platform is established to verify the availability and correctness of the VOT method and the VRM method presented in this paper. Control strategies were tested on the platform and their results compared. The model UR18650ZY of a lithium-ion battery produced by SANYO was utilized in this examination. The specifications are shown in Table 1.

Table 1. Specification of the lithium-ion battery UR18650ZY.

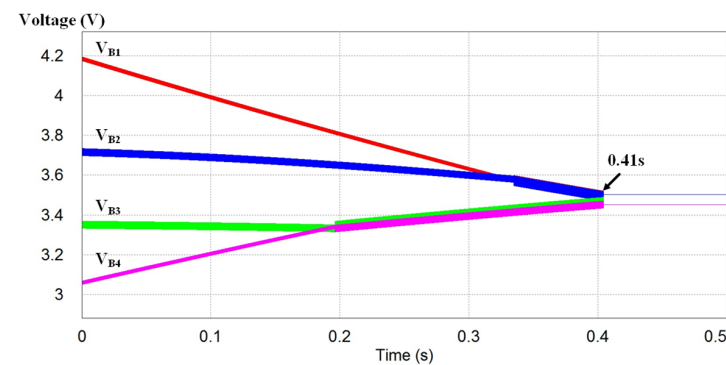
Items	Specification
Type of battery	lithium nickel manganese cobalt oxide battery
Nominal capacity	2600 mAh
Nominal voltage	3.7 V
Max. charging voltage	4.2 V
Min. discharging voltage	3.0 V
Rated charging current	1.25 A
Max. discharging current	5 A

The battery pack was composed of four batteries in series. In order to reduce the complexity and shorten the simulation time, the resistor and capacitor was adopted as the equivalent circuit model of the battery, of which the capacitance was 0.5 F and the internal resistance was 5 mΩ. Table 2 lists the detailed simulation parameters of the bi-directional buck-boost converter. The initial voltages of the four batteries before the balancing process were 4.195 V, 3.715 V, 3.35 V, and 3.05 V, respectively. When the voltage difference between the maximum voltage and the minimum voltage of the batteries was lower than 50 mV, the balancing process was terminated.

Table 2. Simulation parameters of the proposed equalizer.

Items	Value
Inductance (L_m)	7.2 μH
Switching frequency (f_S)	50 kHz
Output capacitance (C_{oss})	169 pF
On-resistance ($R_{DS_{on}}$)	14.5 mΩ

Figure 7a–c are the simulation results of the FDC method, the VOT method, and the VRM method, respectively. Figure 7a–c show that all of three control methods allow the four batteries to reach equilibrium, and the process is terminated as the voltage difference among batteries is within 50 mV. Table 3 is a comparison table of the equilibrium time of the three control methods, and the VRM method saves 31.7% and 26.3% of the time compared with the FDC method and VOT method, respectively.



(a)

Figure 7. Cont.

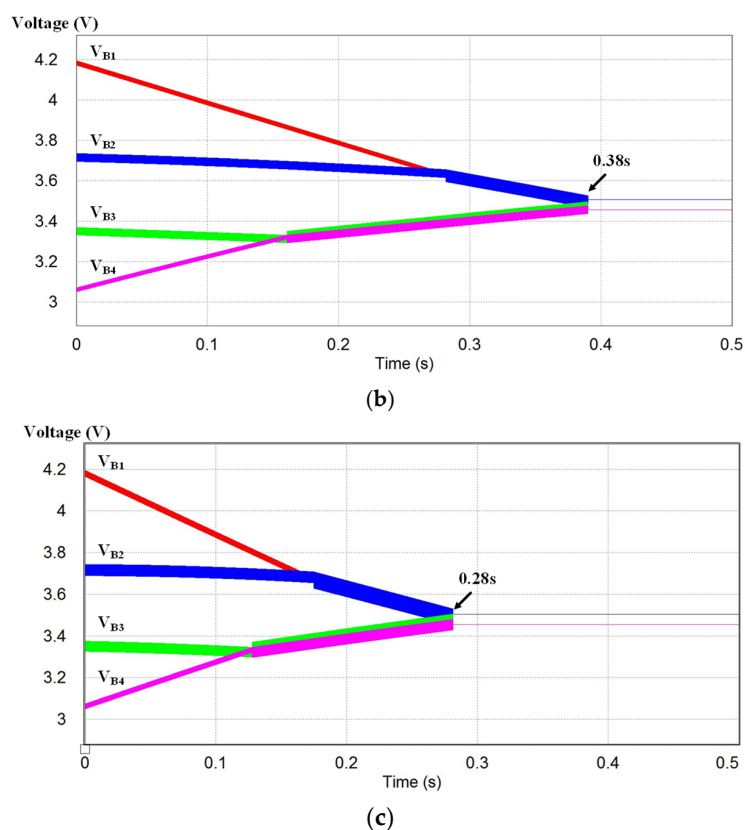


Figure 7. Simulation results of three control strategies: (a) FDC method; (b) VOT method; and (c) VRM method.

Table 3. Comparison of equilibrium time by three control methods.

Method	Before Balance		After Balance	
	ΔV_{diff}		ΔV_{diff}	Elapsed Time
FDC	1.145 V		50 mV	0.41 s
VOT	1.145 V		50 mV	0.38 s
VRM	1.145 V		50 mV	0.28 s

5. Experimental Results and Comparison

According to the simulation parameters, the experimental platform was also built to validate correctness and feasibility. Three bi-directional equalizer circuits with four batteries in series were tested, and corresponding strategies were implemented. Figure 8 and Table 4 show the practical platform of the equalizer system and equipment prepared in the test. In Figure 8, it consists of the bi-directional buck-boost converter, battery pack, Micro-processor which is TMS320F280049 from Texas Instruments Incorporated, voltage sensing and computer interface. The platform could contain non-ideal conditions such as nonlinear component characteristics and temperature changes, which can more precisely verify the feasibility of the proposed control strategies. The comparison results were carried out in different control methods and test conditions with different orders of battery voltage. The balancing procedures of three cases using the three control strategies started with the same initial voltage, and they stopped when the voltage difference between cells was below 50 mV. Table 5 shows the initial voltage conditions of three cases. The main purpose of the examination is that each equalizer can be well controlled according to the voltages of two adjacent batteries, and the proposed VRM method is verified in that it has the shortest equilibrium time under each test condition.

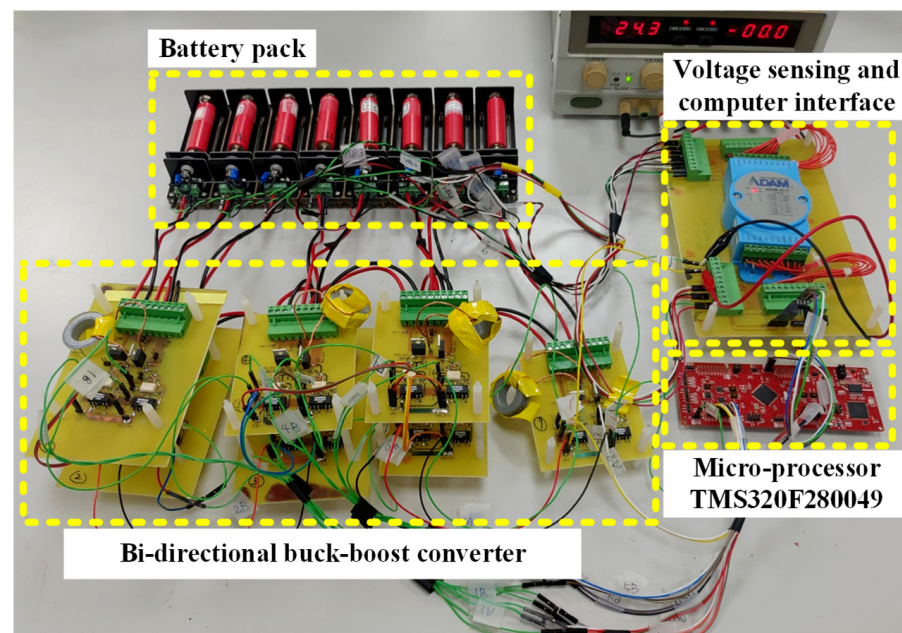


Figure 8. Experimental platform of the equalizer system.

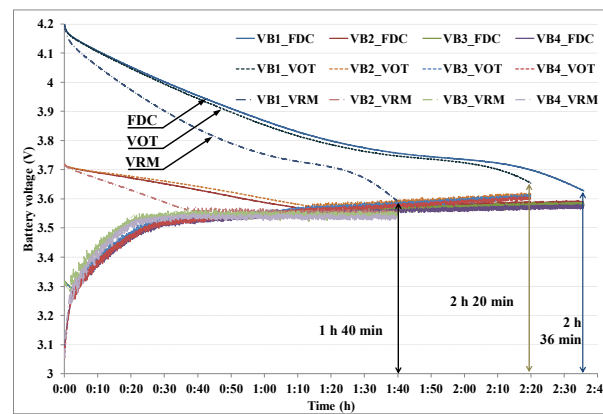
Table 4. Information of equipment prepared in the experiments.

Test Facility	Model
Auxiliary power supply	GPS-4303
Digital scope	HDO8058A
Differential voltage sensing module	ADAM-4117
Differential voltage probe	SI-9002
Current probe	CPL8100A
Micro-processor	TMS320F280049

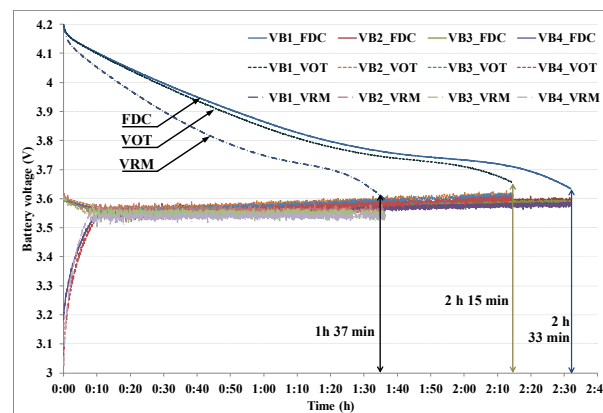
Table 5. Three cases of initial voltage and sequence.

	V_{B1}	V_{B2}	V_{B3}	V_{B4}
Case I	4.196 V	3.716 V	3.315 V	3.06 V
Case II	4.197 V	3.6 V	3.6 V	3.02 V
Case III	3.35 V	4.197 V	3.7 V	3.02 V

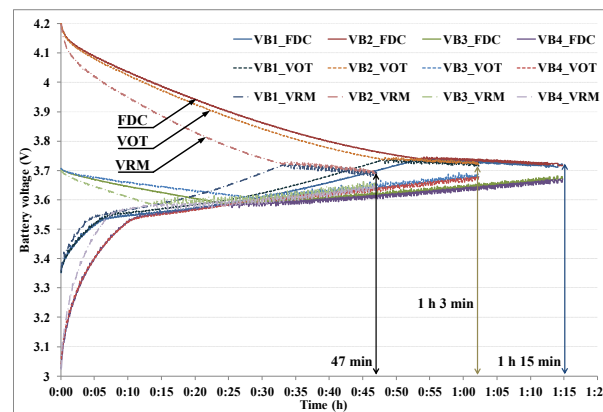
It can be seen from Figure 9 that the energy of the high-SOC battery could be transferred to the low-SOC battery through the buck-boost converter, and the balancing process is completed when the termination condition is reached. From experimental results, it can be inferred that the three control methods are able to exhibit battery balance and the proposed VRM method can achieve equilibrium in the shortest time. Table 6 shows the summarized elapsed time under the three cases. The VOT method calculates the conduction time by Equation (4), which can keep the balancing current at a constant value during the whole balancing time, and its performance is 16% better than the FDC method in case III. The VRM method uses Equations (7) and (8) to obtain the proportion conduction time and cut-off time in a switching period, which means the energy can be further effectively maximized to transfer between two adjacent batteries and speed up equalization. Therefore, the VRM method is the fastest way to reach a balanced condition and it can save 37.3% of equilibrium time compared with the FDC method while in case III.



(a)



(b)



(c)

Figure 9. Measured curves of three cases with three control methods: (a) case I; (b) case II; and (c) case III.

Table 6. Summary table of three cases.

Method	Case I		Case II		Case III	
	Elapsed Time	Saved Time	Elapsed Time	Saved Time	Elapsed Time	Saved Time
FDC	2 h 36 min	-	2 h 33 min	-	1 h 15 min	-
VOT	2 h 20 min	16 min (10.3%)	2 h 15 min	18 min (11.7%)	1 h 03 min	12 min (16%)
VRM	1 h 40 min	56 min (35.9%)	1 h 37 min	56 min (36.6%)	1 h 47 min	28 min (37.3%)

The voltage difference among batteries will significantly rise during the long-term charging or discharging process due to the influence of internal impedance, nonlinear characteristics, and temperature. If the charging or discharging process is stopped early because of unbalance, it will result in lower utilization of the battery cells. Therefore, to verify the proposed equalizer could perform the balancing process while charging and discharging, the tests were carried out during charging and discharging, respectively. Table 7 is a list of battery voltages for charging and discharging test. Each battery voltage was set lower than 4 V initially in the charging test. When the highest voltage among batteries reached 4.2 V, the charger stopped charging. The discharging test was to set the battery voltage higher than 3.6 V initially. Moreover, the charger stopped discharging when the lowest voltage among batteries dropped to 3 V. Figures 10 and 11 are the battery voltage curves under charging and discharging, respectively. The experimental results show that the proposed equalizer can implement battery balancing while charging and discharging situations. The voltage difference among the batteries was within 50 mV after 30 min and the process stopped until any battery voltage reached 4.2 V or dropped to 3 V.

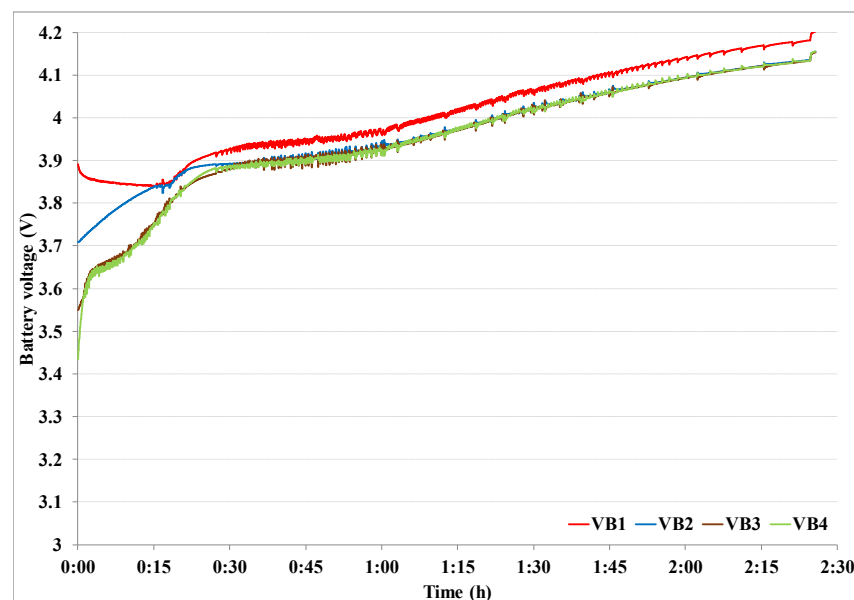


Figure 10. The balancing curves of battery voltage while charging.

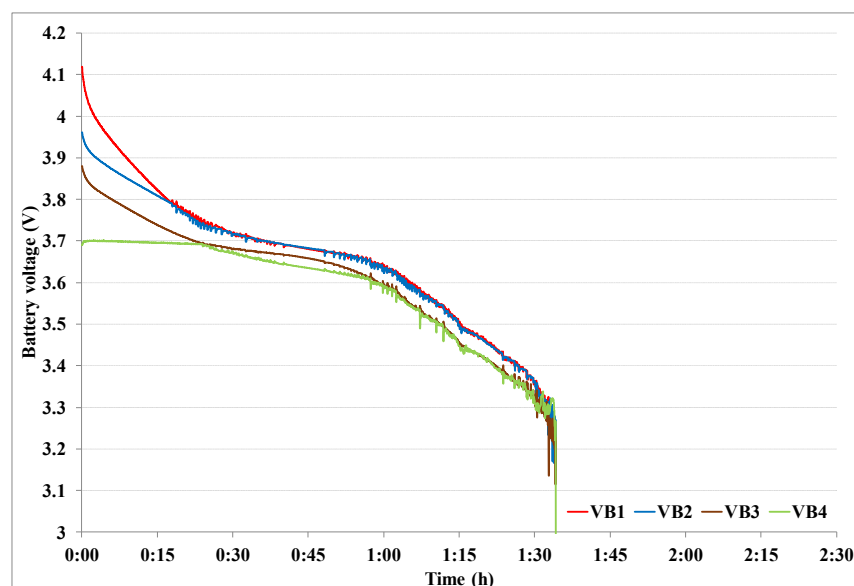


Figure 11. The balancing curves of battery voltage while discharging.

Table 7. Battery voltages while charging and discharging.

Item	Charging		Discharging	
	Before	After	Before	After
V_{B1}	3.891 V	4.200 V	4.119 V	3.262 V
V_{B2}	3.709 V	4.155 V	3.961 V	3.149 V
V_{B3}	3.551 V	4.153 V	3.881 V	3.227 V
V_{B4}	3.434 V	4.155 V	3.692 V	3.000 V

6. Conclusions

This paper develops an active equalizer based on a bi-directional buck-boost converter, featuring a simple scheme, fast balancing speed, and easy implementation compared with other current-controlled equalizers. The proposed equalizer is capable of transferring energy bi-directionally between adjacent cells to make the battery module perform equalization rapidly. The implemented converter is operated in discontinuous conduction mode, so the magnetic component is small and the volume of the equalizer becomes compact. To deal with the problem of decreased balancing current in the later stage of equalization, which results in a prolonged equilibrium period, this paper proposes and realizes two methods, namely, the VOT method and the VRM method, to control the balancing current. The VOT method is able to perform a constant balancing current, while the VRM method enables maximum energy transfer during the entire equalization. The VOT method measures the voltage of the high-SOC battery to obtain the conduction time of the main switch; thus, the balancing current can be maintained at a constant value. However, the VOT method only detects the voltage of the high-SOC battery. It cannot take the low-SOC battery into account to dispatch the optimal proportion of the conduction time and the cut-off time in a switching period. Therefore, the VRM method is presented to use the voltages of the adjacent batteries in the described equation to calculate conduction time and cut-off time, which makes the energy transferring time almost fill up the entire switching period, and maximize the balancing current for the equalizer. The simulations and experiments are established to verify the proposed control methods. According to experimental results, the VOT method is validated to solve the reduced balancing current during the later equalization process and shortens the equilibrium time by 10.3%, 11.7%, and 16% compared with the conventional method. The VRM method is able to maximize the balancing current in the whole equalization process and shortens the equilibrium time by 35.9%, 36.6%, and 37.3% compared with conventional method. Furthermore, in the process of charging and discharging tests, the active equalizer proposed in this paper is verified to achieve equilibrium successfully. Finally, in future studies, the battery SOC could be considered and the long-term cycle life test could be performed to demonstrate the effectiveness of the proposed methods.

Funding: This research was funded by Ministry of Science and Technology, grant number MOST 110-2221-E-131-015—and the APC was funded by Ming Chi University of Technology.

Institutional Review Board Statement: Not applicable.

Informed Consent Statement: Not applicable.

Data Availability Statement: Not applicable.

Conflicts of Interest: The authors declare no conflict of interest.

References

1. Kwon, S.-J.; Lee, S.-E.; Lim, J.-H.; Choi, J.; Kim, J. Performance and Life Degradation Characteristics Analysis of NCM LIB for BESS. *Electronics* **2018**, *7*, 406. [[CrossRef](#)]
2. Ali, M.; Zafar, A.; Nengroo, S.; Hussain, S.; Kim, H. Effect of Sensors Sensitivity on Lithium-Ion Battery Modeled Parameters and State of Charge: A Comparative Study. *Electronics* **2019**, *8*, 709. [[CrossRef](#)]

3. Go, S.-I.; Choi, J.-H. Design and Dynamic Modelling of PV-Battery Hybrid Systems for Custom Electromagnetic Transient Simulation. *Electronics* **2020**, *9*, 1651. [\[CrossRef\]](#)
4. Stan, A.; Świerczyński, M.; Stroe, D.; Teodorescu, R.; Andreasen, S.J. Lithium ion battery chemistries from renewable energy storage to automotive and back-up power applications—An overview. In Proceedings of the 2014 International Conference on Optimization of Electrical and Electronic Equipment (OPTIM), Bran, Romania, 22–24 May 2014; pp. 713–720.
5. Affanni, A.; Bellini, A.; Franceschini, G.; Guglielmi, P.; Tassoni, C. Battery choice and management for new-generation electric vehicles. *IEEE Trans. Ind. Electron.* **2005**, *52*, 1343–1349. [\[CrossRef\]](#)
6. Aiello, O. Electromagnetic Susceptibility of Battery Management Systems' ICs for Electric Vehicles: Experimental Study. *Electronics* **2020**, *9*, 510. [\[CrossRef\]](#)
7. Barzkar, A.; Mohammad, S.; Hosseini, H. A novel peak load shaving algorithm via real-time battery scheduling for residential distributed energy storage systems. *Int. J. Energy Res.* **2018**, *42*, 2400–2416. [\[CrossRef\]](#)
8. Lukic, S.M.; Cao, J.; Bansal, R.C.; Rodriguez, F.; Emadi, A. Energy Storage Systems for Automotive Applications. *IEEE Trans. Ind. Electron.* **2008**, *55*, 2258–2267. [\[CrossRef\]](#)
9. Lawder, M.T.; Suthar, B.; Northrop, P.W.; De, S.; Hoff, C.M.; Leitermann, O.; Crow, M.L.; Santhanagopalan, S.; Subramanian, V.R. Battery energy storage system (BESS) and battery management system (BMS) for grid-scale applications. *Proc. IEEE* **2014**, *102*, 1014–1030. [\[CrossRef\]](#)
10. Baronti, F.; Bernardeschi, C.; Cassano, L.; Domenici, A.; Roncella, R.; Saletti, R. Design and safety verification of a distributed charge equalizer for modular Li-ion batteries. *IEEE Trans. Ind. Inform.* **2014**, *10*, 1003–1011. [\[CrossRef\]](#)
11. Krein, P.T.; Balog, R.S. Life Extension Through Charge Equalization of Lead-Acid Batteries. In Proceedings of the 24th Annual International Telecommunications Energy Conference (INTELEC), Montreal, QC, Canada, 29 September–3 October 2002; pp. 516–523.
12. Zheng, Y.; He, F.; Wang, W. A Method to Identify Lithium Battery Parameters and Estimate SOC Based on Different Temperatures and Driving Conditions. *Electronics* **2019**, *8*, 1391. [\[CrossRef\]](#)
13. West, S.; Krein, P.T. Equalization of Valve-Regulated Lead-Acid Batteries: Issues and Life Test Result. In Proceedings of the 22nd International Telecommunications Energy Conference, Phoenix, AZ, USA, 10–14 September 2000; pp. 439–446.
14. Kutkut, N.H.; Wiegman, H.L.N.; Divan, D.M.; Novotny, D.W. Design Considerations for Charge Equalization of an Electric Vehicle Battery System. *IEEE Symp. Ind. Electron. Appl.* **1999**, *35*, 28–35. [\[CrossRef\]](#)
15. Hong, S.; Jiang, J.; Li, X. A battery management system with two-stage equalization. In Proceedings of the 29th Chinese Control and Decision Conference, Chongqing, China, 28–30 May 2017.
16. Oman, H. Making Batteries Last Longer. *IEEE Aerosp. Electr. Syst. Mag.* **1999**, *14*, 19–21.
17. Kim, J.; Shin, J.; Chun, C.; Cho, B.H. Stable configuration of a Li-ion series battery pack based on a screening process for improved voltage/SOC balancing. *IEEE Trans. Power Electron.* **2012**, *27*, 411–424. [\[CrossRef\]](#)
18. Luo, W.; Jie, L.; Song, W.; Feng, Z. Study on passive balancing characteristics of serially connected lithium-ion battery string. In Proceedings of the 13th International Conference on Electronic Measurement & Instruments, Yangzhou, China, 20–22 October 2017.
19. Ke, W.; Zhang, N. Passive Equalization and the Expiration of Battery Packs on Chinese Electric Bicycles. In Proceedings of the 2nd IEEE Conference Industrial Electronics and Applications, Harbin, China, 23–25 May 2007; pp. 1370–1373.
20. Lu, L.; Han, X.; Li, J.; Hua, J.; Ouyang, M. A review on the key issues for lithium-ion battery management in electric vehicles. *J. Power Sources* **2013**, *226*, 272–288. [\[CrossRef\]](#)
21. Carter, J.; Fan, Z.; Cao, J. Cell equalization circuits: A review. *J. Power Sources* **2020**, *448*, 227489. [\[CrossRef\]](#)
22. Li, J.; Zhou, S.; Han, Y. Mathematical modeling, performance analysis, and control of battery equalization systems: Review and recent developments. *IEEE Adv. Battery Manuf. Serv. Manag. Syst.* **2017**, *12*, 281–302.
23. Gallardo-Lozano, J.; Romero-Cadaval, E.; Milanés-Montero, M.I.; Guerrero-Martinez, M.A. Battery equalization active methods. *J. Power Sources* **2014**, *246*, 934–949. [\[CrossRef\]](#)
24. Ye, Y.; Cheng, K.W.E. An Automatic Switched-Capacitor Cell Balancing Circuit for Series-Connected Battery Strings. *Energies* **2016**, *9*, 138. [\[CrossRef\]](#)
25. Kim, M.Y.; Kim, C.H.; Kim, J.H.; Moon, G.W. A Chain Structure of Switched Capacitor for Improved Cell Balancing Speed of Lithium-Ion Batteries. *IEEE Trans. Ind. Electron.* **2014**, *61*, 3989–3999. [\[CrossRef\]](#)
26. Shi, F.; Song, D. A Novel High-Efficiency Double-Input Bidirectional DC/DC Converter for Battery Cell-Voltage Equalizer with Flyback Transformer. *Electronics* **2019**, *8*, 1426. [\[CrossRef\]](#)
27. Farzan Moghaddam, A.; Van den Bossche, A. Forward Converter Current Fed Equalizer for Lithium Based Batteries in Ultralight Electrical Vehicles. *Electronics* **2019**, *8*, 408. [\[CrossRef\]](#)
28. Park, S.H.; Kim, T.S.; Park, J.S.; Moon, G.W. A new battery equalizer based on buck-boost topology. In Proceedings of the IEEE 7th International Conference on Power Electronics, Daegu, Korea, 22–26 October 2007; pp. 962–965.
29. Dong, B.; Li, Y.; Han, Y. Parallel Architecture for Battery Charge Equalization. *IEEE Trans. Power Electron.* **2015**, *30*, 4906–4913. [\[CrossRef\]](#)
30. Ji, W.; Lu, X.; Ji, Y.; Tang, Y.; Ran, F.; Peng, F.Z. Low cost battery equalizer using buck-boost and series LC converter with synchronous phase-shift control. In Proceedings of the 2013 Twenty-Eighth Annual IEEE Applied Power Electronics Conference and Exposition, Long Beach, CA, USA, 17–21 March 2013; pp. 1152–1157.

31. Lee, Y.S.; Chen, G.T. ZCS bi-directional DC-to-DC converter application in battery equalization for electric vehicles. *IEEE J. Emerg. Sel. Top. Power Electron.* **2004**, *4*, 2766–2772.
32. Lee, Y.S.; Chen, G.T. Quasi-Resonant Zero-Current-Switching Bidirectional Converter for Battery Equalization Applications. *IEEE Trans. Power Electron.* **2006**, *21*, 1213–1224. [[CrossRef](#)]
33. Wang, S.C.; Liu, C.Y.; Liu, Y.H. A Non-Dissipative Equalizer with Fast Energy Transfer Based on Adaptive Balancing Current Control. *Electronics* **2020**, *9*, 1990. [[CrossRef](#)]
34. Wang, S.C.; Chen, G.J.; Liu, Y.H.; Luo, Y.F.; Yang, Z.Z. An active balancer with rapid bidirectional charge shuttling and adaptive equalization current control for lithium-ion battery strings. *Int. J. Energy Res.* **2020**, *46*, 223–238. [[CrossRef](#)]
35. Wang, S.C.; Liu, C.Y.; Liu, Y.H. A Fast Equalizer with Adaptive Balancing Current Control. *Energies* **2018**, *11*, 1052. [[CrossRef](#)]